INDONESIAN JOURNAL ON GEOSCIENCE
Geological Agency
Ministry of Energy and Mineral Resources

Journal homepage: http://ijog.geologi.esdm.go.id
ISSN 2355-9314, e-ISSN 2355-9306

The Weighted Values of the Factor's Classes Based on Different Approaches for Potential Zones of the Groundwater Mapping Using Remote Sensing Data and GIS Technique in the Taiz Region, Yemen

Anwar Abdullah[1], and Ahmed Abdul Aziz[1], and Zulherry Isnain[2]

[1]Geology Department, Faculty of Applied Sciences, Taiz University, Taiz, Yemen
[2]Geology Programme, Faculty of Science and Natural Resources, Universiti Malaysia Sabah, Sabah, Malaysia

Corresponding author: zulherry@gmail.com
Manuscript received: March, 05, 2024; revised: November, 11, 2024;
approved: September, December, 03, 2024; available online: April, 24, 2025

Abstract - Remote sensing and geographical information system (GIS) have become one of the leading tools in the field of groundwater, which help in assessing, monitoring, and mapping groundwater resources, especially in semi-arid areas. The objective of this paper is to assess and to map groundwater potential zone in Taiz Governorate by the overlaying technique of the geospatial factors. The available twelve factors were prepared in this work from different data sources using several processes. The soil and landuse factors were prepared from Landsat-7 with the colour enhancement technique and supervised classification. The lineament, automatic drainage, slope, elevation steepness (topography) and aspect were derived from DEM, rock units, geological faults, and contact created from previous geological map. Geophysical subsurface faults were also prepared from previous magnetic faults. The rainfall data was generated from the previous annual rainfall reading. All these maps were prepared and classified to be suitable for weighted values and GIS overlying model. The manual, scaling, and matrix weighted values were assigned to the factor (raster) maps to produce three groundwater potential zone maps. These maps were classified into five classes as very low, low moderate, high, and very high potential zones. Three groundwater potential maps produced in this work were compared together and evaluated using matching technique with previous prospecting groundwater map. The percentages of the matching were 58.56 % for the potential map of the matrix analysis, 27.95 % for the potential map of the scaling equation, and 13.49 % for the potential map of the manual weighted values. This evaluation shows that the potential map of matrix weighted values scored the highest of matching, and it is the best potential map compared with the other two maps. The new finding in this work was more than six new places in the best groundwater potential map of the area noted as new groundwater potential areas. The locations of these areas were NE corner, S-SW, W, NW corner, N, and some places in the central parts of the studied area. Hence, the resultant map may contribute to optimize the choice of location of future drilling, and to increase the chances to take water from new wells which will satisfy the increasing water demand of local population. Moreover, the groundwater potential zone map was assessed for the first time using these techniques in the area, and all maps of the factors created in this research are new maps that may represent the new database of the area.

Keywords: groundwater, mapping, weighted values, overlying, evaluation

How to cite this article:
Abdullah, A., Aziz, A.A., and Isnain, Z., 2025. The Weighted Values of the Factor's Classes Based on Different Approaches for Potential Zones of the Groundwater Mapping Using Remote Sensing Data and GIS Technique in the Taiz Region, Yemen. *Indonesian Journal on Geoscience*, 12 (1), p.105-131. DOI: 10.17014/ ijog.12.1.105-131

Introduction

Water is one of the most vital natural resources for all life on earth. The availability and quality of water have always played an important part in determining not only where people can live, but also their quality of life. Water must be considered as a finite resource that has limits and boundaries to its availability and suitability for use (Encyclopedia, 2022). The water crisis in Taiz region has

the potential to destroy human and plant lives. The water crisis was triggered by a sharp population increase, misguided agricultural policies promoting the use of water, a lack of governmental regulation on using water, and a vulnerable climate to global warming (Glass, 2010). The situation in Yemen country stands out, however, among other arid to semi-arid countries. Yemen is one of the poorest countries in the world, where the critical water situation in Taiz has not received the attention of the government organizations. It will not be possible to approach a realistic solution in a short time. In general, the ground (shallow) and surface water resources in Taiz region undergo increasing pressure caused by the expanding population, and agricultural activities. These water resources are mostly recharged by the water during the rainy season (summer). While during dry seasons, water shortage due to various activities leads to a water crisis in the area. For this reason, the current study attempts to assess and to map the potential areas of groundwater availability in Taiz area using the remote sensing and geographic information system (GIS) techniques. The studied area in this work is located in the south-southwestern of The Republic of Yemen (Figure 1), between latitudes 1457514 N and 1533166 N, and longitudes 355108 E and 436467 E. It is about 6,725 km^2. In general, the topography of the area is characterized by high irregular mountains where elevation varies from 1,000 m to 3,600 m situated at the most parts of Taiz region with numerous small hills. There are several valleys (wadis) covered by some vegetation.

According to Aneesh and Deka (2015), the definition of the ground-water potential recharge zone is the most important natural resource found beneath the earth surface stored in void space of geological stratum used in economic development, domestic life, and any ecological diversity. Also, they conclude the occurrence and flow system of groundwater depends on the geological characteristics of its porosity and permeability, the formation of landforms, and the role of landforms on surface runoff and infiltration to the ground. Rajaveni *et al.* (2015) also define groundwater recharge; it is the percolation and/or infiltration of water from an unsaturated zone (surface) to a saturated zone through porosity and permeability of the earth materials above the water table. It finalizes precipitation, infiltration and/or percolation of the surface water to the subsurface influenced by geology and geomorphology.

Water scarcity is a well-known problem, especially in arid to semi-arid areas. Through the most recent couple of decades, a great interest in utilizing remote sensing (RS) and geographical information system (GIS) techniques for groundwater potential zones has been made by many researchers all over the world. The groundwater

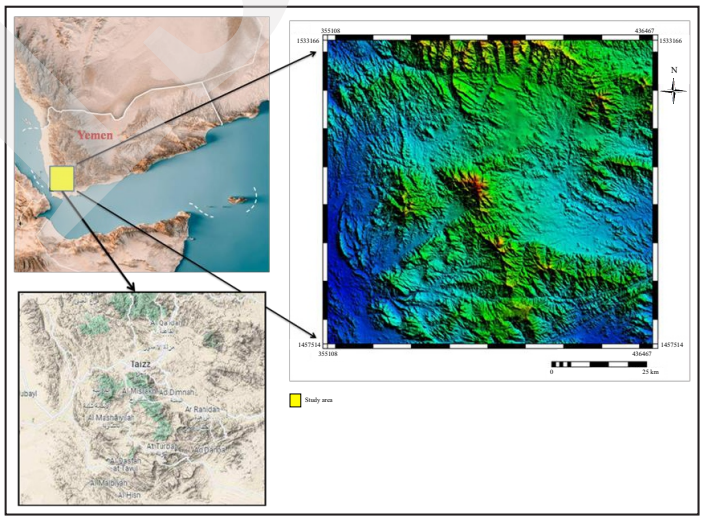

Figure 1. Location of the studied area.

potential zones must be delineated through different geospatial thematic layers (Shekhar and Pandey, 2015). The use and the mapping of groundwater resources need to understand the geospatial factors of any area. The preparation of different geospatial factor maps as thematic maps of the ground area from different data sources is helpful for mapping groundwater potential zones (Isnain and Musta, 2022). Mapping groundwater potential zones is essential for the construction and planning of the location of new abstraction wells to meet the increasing water demand. The occurrence, distribution, and movement of groundwater are controlled by geological and geomorphological features of the area (Kumar *et al*., 2016). The remote sensing satellite data is a useful tool for providing rapid and costly groundwater information from the various factors controlling directly or indirectly the presence and the movement of groundwater (Jha *et al.*, 2007). The geographic information system (GIS) has also proved to be a useful tool for groundwater studies, due to its capability in handling large and complex spatial data for resource management and decision making (Stafford, 1991). The groundwater potential resources of any region are mostly influenced by the aquifer characteristic that primarily depends on the earth natural resources like geology, geomorphology, soil, slope drainage, and lineament (Shekhar and Pandey, 2014).

There are many methods used to prepare groundwater potential zones mainly based on the information of the surface and subsurface surveys. The advent technology of remote sensing and geographical information system (GIS) technologies for groundwater potential zone mapping using different geospatial data has become an easy procedure (Isnain and Mokthar, 2022). Various factors such as soil, landuse, lineaments, geology, elevation, steep-ness, rainfall, and drainage mapped from different sources of data are taken for mapping of groundwater zones (Isnain and Mokthar, 2022; Isnain and Musta, 2022). Moreover, the GIS technique was used to classify the results of remote sensing, assigning the appropriate weights to the related maps. These factor maps were used to identify the groundwater flow and recharge zones (Salwa, 2015; Sciences, 2013). In this study, the groundwater conditions vary significantly depending upon the different geo-spatial data such as elevation steepness, slope, aspect, drainages, lineaments, soil, landuse, rock units, geological faults, contact of rock bodies, subsurface faults (geophysical faults), and annual rainfall. These factor data can be created from satellite images and DEM digital elevation model, previous geological, geophysical (magnetic), and annual rainfall reading of the ten past year data. The different processes were used to prepare, to analyze, and to interpret these factors with different weighted values for the groundwater potential zone area mapping through the GIS overlay technique.

Materials and Methods

Different data and methods were used in this work for groundwater potential zone mapping by the remote sensing and geographic information system (GIS) in the studied area (Figure 2). As far as this study is concerned, it was used for the first time to delineate the potential areas of the groundwater in the Taiz region by the techniques.

Data and Processing

Different sources of data were used in this work to create the factor layers or maps, such as elevation steepness, slope, aspect, drainages, lineaments, soil, landuse, rock units, geological faults, contact of rock bodies, subsurface faults (geophysical faults), and annual rainfall. These factors can be created from digital data of remote sensing and DEM digital elevation model, previous geological, geophysical (magnetic), and annual rainfall reading of the past ten year data, respectively. These twelve thematic maps of factors were used in this work based on the available data, and were taken into consideration after deep literature reviews along with field expert advice.

During this study, many different software packages were used, since there was no single

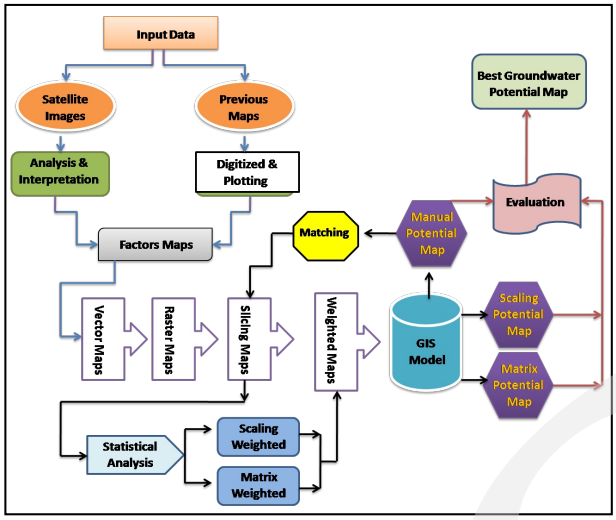

Figure 2. Flow chart of methodology in the study.

software that would process all steps in the analyses. Therefore, the diverse software used for the analysis in the current study are PCI Geomatica (version 9.1), ERDAS (version 8.4), Global Mapper (version 8), and ILWIS (version 3.4).

Satellite Landsat-7 (ETM) Image Data

Satellite data such Landsat-7 Enhance Thematic Mapper (ETM) is one of the NASA satellite series that was launched in 1999 into space. Two Landsat-7 Satellite Image (ETM) scenes acquired on 4th Jun 2008, with paths165-166 and rows 51-51 were used in this study. These images were enhanced with different processing techniques to produce the landuse and soil factor maps. The studied area was not found in one image, but all the area was found in two satellite images of Landsat-7 (ETM). These images were mosaiced to produce one image. Then, the subset image technique was used in the studied area. The ERDAS 8.4 software was used to apply the mosaic and subset image techniques. Geometric correction has been done with the WGS 84 projection and Universal Transverse Mercator, Yemen, by using ground control points (or GCPs) in the distorted image and by matching them to their true positions in the topographic map coordinates. Atmospheric correction is one of the radiometric enhancement techniques applied in this study, used to examine the observed brightness values (Digital Numbers) (Gupta, 2013; Jensen, 2005; Jensen, 1996). For this purpose, median filter and contrast enhancement techniques have been applied to the satellite images of the studied area. The median filter is useful for noise suppression in any image as it is an edge-preserving filter. It is also applicable in removing pulse function noise, which results from the inherent pulsing of microwaves. Version 9.1 of PCI Geomatica image processing software was used to apply 3 by 3 median filter kernel sizes within software packages. The histogram equalization technique was applied to the different satellite imageries of the studied area. This technique can also be used to minimize the effect of haze. For most conventional remote sensing systems, it ranges between extreme dark (0) and the high end to the extreme white (255).

A multispectral image consists of several bands of data. Each band of the image contains a different amount of spectral information about the features on the surface based on the wave length (Jensen, 1996). Colour enhancement is generated by assigning three bands or components to the primary colours of red, green, and blue (RGB). Generally, the coloured image presentation improves the display of differences in patterns such as topographic units, vegetation types, and drainage valley boundaries. This false colour combination and analysis made it easier to identify landuse patterns of natural or man-

made features, geologic formation boundaries, and types of soils based on tonal changes. Colour composites are useful for image interpretation since the information from three spectral bands may be displayed simultaneously, and the signature of certain features can be strengthened depending on which components were chosen for combination (Gupta and Srivastava, 2010; Chen and Campagna, 2009). False colour images were produced for landuse and soil mapping, because they increased the interpretability of the data. The seven bands of the Landsat-7 (ETM) of the studied area were used to produce more than 140 coloured images.

Several researchers, such as Avtar *et al*. (2010) and Adiat *et al*. (2012) have already mentioned the importance of different geospatial factors such as geology, landuse, slope, soil, drainage density, surface annual rainfall, *etc*., controlling groundwater potential of any area. However, the extent to which they affect it, may differ from place and time. Reservations in mapping discharge and recharge relations across large areas include the temporal variability, affected by both seasonal and long term such as climate and landuse changes, and local scale variations in the controls on preferential flow (Sarah *et al*., 2006). The landuse map tells the information about the soil moisture, infiltration, groundwater, and surface water. Whereas the soil is the most important factor that determines the infiltration capacity of the region.

In this work, 147 coloured images were compared to each other based on the ability of the coloured images to identify the landuse features and types of soils with a reference to the previous landuse and soil maps (part maps) of the studied area. Also it is based on field observations and user experience. The colour composition image of the 4, 3, and 2 bands as red, green, and blue shows the best coloured image in this study in terms of landuse identification as shown in Figure 3. This image was used to create the landuse map of the studied area by the supervised classification technique. Moreover, the coloured images of the 7, 4, 1 band as red, green, and blue was found as the best coloured image for determining the different types of soils (Figure 4). The supervised classification technique was used to classify the different land features from the coloured images of the 4, 3, 2 bands based on the intensity reflection (digital number) of the objects within ERDAS 8.4

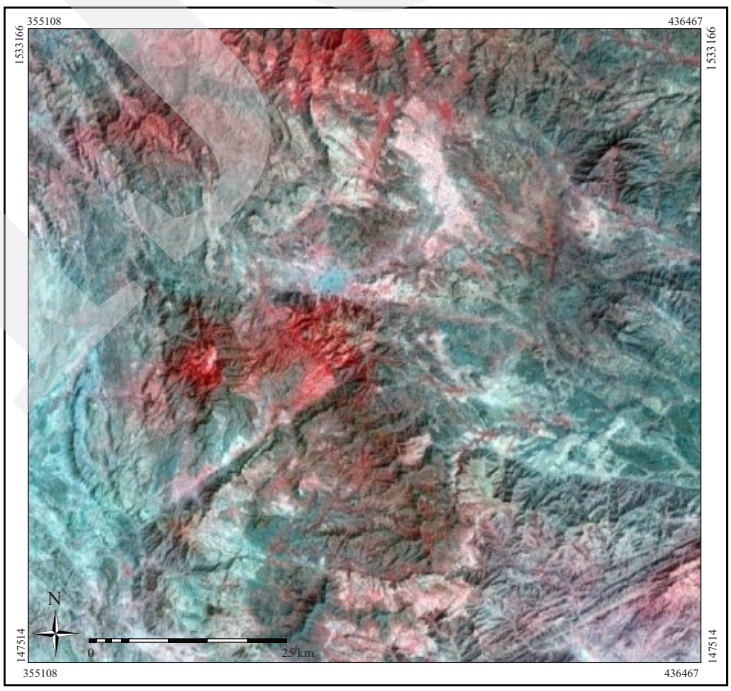

Figure 3. Coloured image of 432 band combination, in terms of landuse identification.

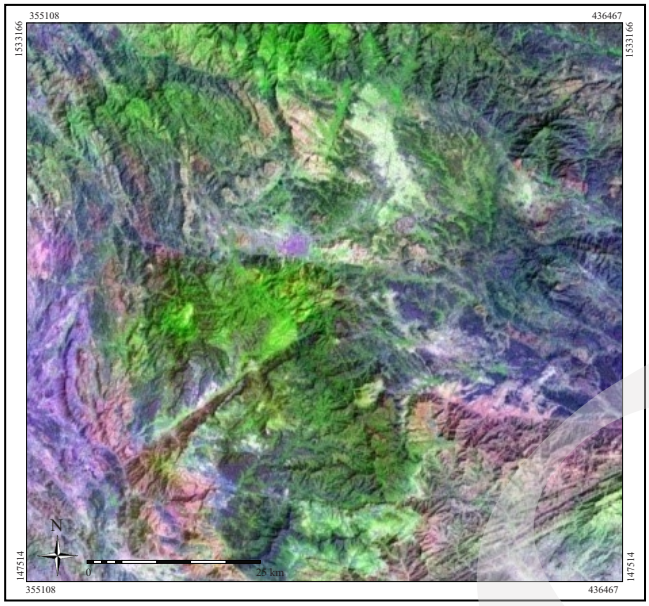

Figure 4. Coloured image of 741 band combination, for determining the different types of soils.

software package. The supervised classification technique was used to classify the different types of soils from the coloured images based on the intensity reflection (digital number) of the objects within ERDAS 8.4 software package.

In this classification, only twenty-five pixels with the same intensity reflection for each class were selected. Then, similar pixels were automatically determined to produce the class in the whole images. Four different classes of landuse and three different classes of soil were identified from satellite-coloured images of 4, 3, 2 and 7, 4, 1 band combinations, respectively. After image classifications, the digitizing technique was used by the ILWIS software to produce the landuse and soil maps separately.

Digital Elevation Model (DEM) Data

Digital Elevation Model (DEM) generally refers to a regular array of elevations (squares), and is represented as a rasteror grid map. Each cell in the grid has its own elevation value (Ross and Beljin, 1994).

Topographical surface investigations include the delineation and the mapping of various landforms such as slope, aspect, and drainage parameters that could have a direct control on the occurrence and the flow of groundwater (Waikar and Nilawar, 2014; Solomon and Ghebbreab, 2008; Sreedevi *et al*., 2005). The mapping activities significantly contribute to deciphering areas of groundwater recharge and their potential for groundwater development (Singhal and Gupta, 1999). The geomorphology of an area is an important factor in assessing the groundwater potential and prospect, because it controls the subsurface movement of groundwater (Kumar *et al*., 2008). A digital elevation model (DEM) was used to generate topographical or geo-morphological parameters of the studied area.

To identify groundwater potential zones in the studied area, factors influencing the groundwater potential were prepared using DEM data. Five parameters have been created from DEM data in this study. The factors (parameters) were elevation steepness, drainage, slope, lineament, and aspect (flow direction) that were used in this research. The DEM was generated from topographic maps of the area with a scale of 1:50,000 by digitizing the technique of a 30 m contour line using PCIGeomatica 9.1. Then, the fusion technique for DEM with Landsat-7 satellite images was also used to improve the resolution and the appearance of the features of the DEM. The final resolution of the DEM was set to 30 m.

The elevation steepness (topographic elevation) is the altitude changes of the elevation for the surface area above sea level. The highest elevation areas have a low significant impact on the occurrence and the movement of the surface water to recharge the groundwater. Whereas the lowest elevation areas have a high significant impact on the occurrence and the movement of the surface water to recharge the groundwater. The elevation steepness factor of the area was generated from DEM using interpolation of the contour lines with elevation values by the ILWIS 4.3 software package.

The drainage basin is the natural draining of water runoff to lowlands or to a common point. The drainage density and the type of drainage indicate the information on rock and soil permeability, infiltration of water, and surface runoff (Manap, 2013; Horton, 1945). The drainage density is the measure of the total line length of the stream network to the total basin area. This is important in identifying the nature of the drainage basin. The highly dense streams usually indicate the texture of a mature, well-developed channel system with limited infiltration and high runoff, that indicate the behaviour of surface and subsurface formation, the information of rock, soil permeability, infiltration of water, and surface runoff (Das *et al*., 2012; Abdullah *et al*., 2013; Babu *et al*., 2014). The automatic drainage map was derived from the DEM data using PCIGeomatica 9.1 software, and the drainage map was composed by taking into account the length of drainage per meter area. The minimum length of the drainage was considered as 50 m, and the thresholds of the pixels were also 50. The drainage density was prepared from drainage network map by hydro-processing tool of ILWIS 4.3, and reclassified into five categories.

Lineaments are linear features on the earth surface that reflect a general surface expression of underground fractures (Abdullah *et al*., 2010; Pradhan *et al*., 2006). Lineaments are geological linear or curvilinear features that are the zone of fractured bedrocks with a high-groundwater prospect (Shekhar and Pandey, 2015; Rao and Jugran, 2003; Nassr and Abdullah, 2015), resulted from faulting and fracturing, and hence are the zone of amplified porosity and permeability. Lineament mapping in a hard rock terrain is very beneficial because of their influence in the storage and movement of groundwater by these linear features (Thapa *et al*., 2017). According to Abdullah *et al*. (2013) and Thapa *et al*. (2017) the studied area is considered as an active tectonic area (rifting zone area) as well based on the field observations and user experiences. In this work, lineaments are interpreted fractures related to the structural weakness, where non-geological was not considered. The DEM data was used to create the gradient shader image by the Global Mapper 8.0 software. The histogram equalization technique was applied to this image to enhance the linear features (lineaments) in the area as shown in Figure 5. The lineament map was created from gradient shader using the ILWIS software.

Aspect is the compass direction that a topographic slope faces, usually measured in degrees from north. Aspect can be generated from continuous elevation surfaces. For example, the aspect recorded for a DEM face is the steepest down-slope direction of the face, and the aspect of a cell in a raster is the steepest down-slope direction of a plane defined by the cell and its eight surrounding neighbours (Gupta and Srivastava, 2010).

The dominant face direction could relate to the flat or near to flat areas. The high dominant face direction areas may refer to the high infiltration rate of the surface water toward the groundwater. The aspect map of the area was generated from DEM using DEM hydro-processing technique of the ILWIS software package.

The slope layer was created also from DEM using equation. This equation was typed in an expression on the command line of the ILWIS software. The slope map was sliced into five various classes based on the degrees of different slopes in the area. The gentle slope indicates the presence of very high groundwater potential zones, whereas the steep slope shows the presence of low groundwater potential zones as water runs rapidly off the surface, and does not have sufficient time to infiltrate the surface (Todd, 2005).

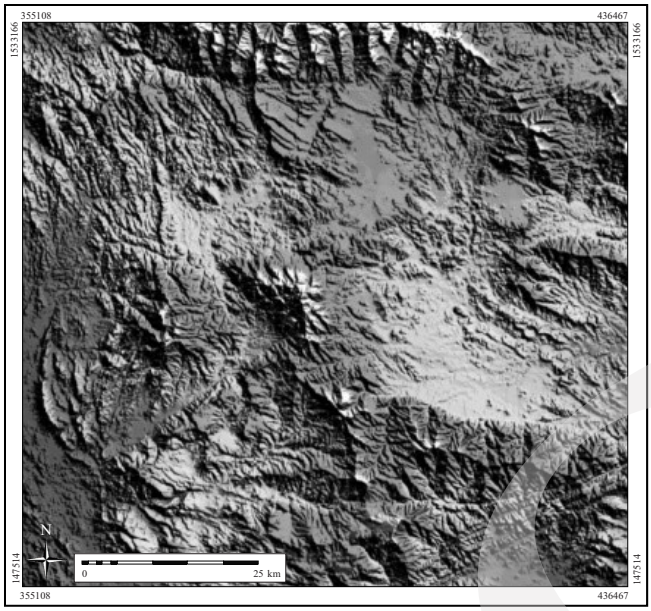

Figure 5. Gradient shader created from DEM of the studied area.

Geological and Geophysical Data

Parameters influencing ground-water potential and recharge and their relative importance are taken from previous literature such as geological and geophysical maps of the area. A study by different researchers such as Ruiz *et al*. (2010), Shaban *et al*. (2006), Pradhan (2009), Sciences (2013) assigned that the rock units and geological faults are major important factors for groundwater potential zone mapping. The geology of an area is one of the key factors in groundwater potential zone delimitation. Various geological formations have different water bearing capacities and subsurface flow characteristics based on their porosity, permeability, and fractures. Geological structures like surface faults and subsurface faults are known to impact the groundwater as they control vertical and horizontal water movement within the geological formations (Shaban *et al*., 2006; Wakgari, 2010). The rock unit (geology) and surface or subsurface faults exposed to the surface are highly affect the groundwater recharge by controlling the percolation and flow of water to the ground, and play a great role in the occurrence and distribution of groundwater potential zones.

The contact between two lithologies can also appear as a linear feature. This contact may show as a change in the drainage pattern across the lineament (Brockmann *et al*., 1977), or the two units may have different spectral properties (Nguyen and Ho, 1988). Regarding to this definition, the contact of the rock units was used in this work as one of the factors that may play an important role in recharging the groundwater by the surface water.

The rock units, geological faults and contact were taken into consideration in this study. Geology is important for knowing the occurrence of groundwater. The rock unit, fault, and contact maps were created by digitizing process by ILWIS3.4 from the geological map of scale 1:250,000 produced by the geological survey of Yemen 1990 (GSY, 1991) (Figure 6).

Faults are the primary indicators of secondary porosity and also for potential sources of water supply. The fault and contact maps were converted into fault density map and contact buffer map as shown in Figures 7 and 8, respectively. Accordingly, areas with high fault density and less buffering are able to drain the rain faster than those with low density. This implies that areas with high fault density and low buffering contact are favourable for groundwater. Whereas, their counter-parts with low density and high buffering are unfavourable for it (Gupta and Srivastava, 2010; Todd, 2005).

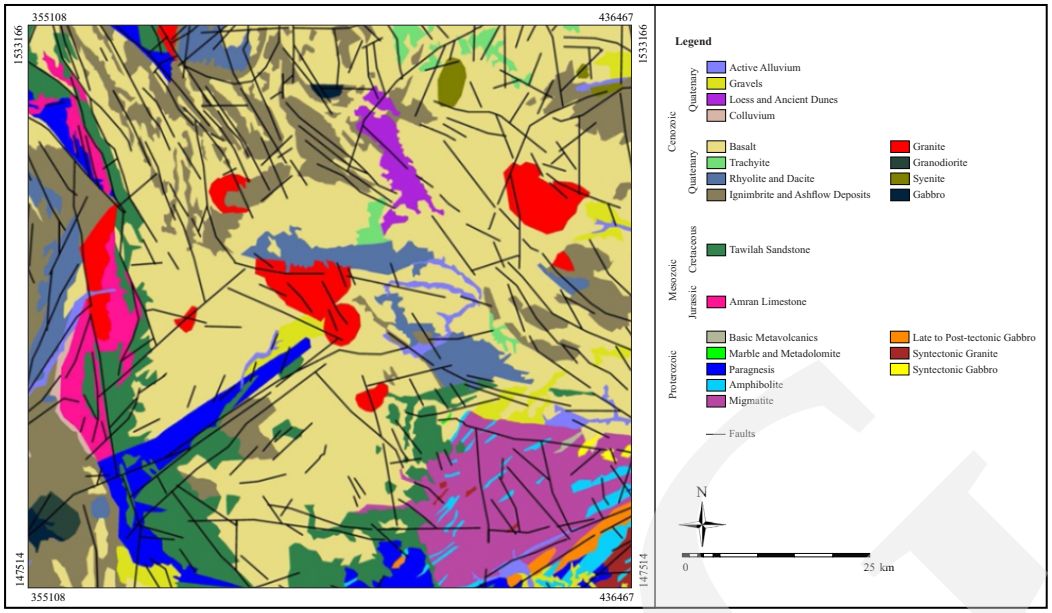

Figure 6. Geological map with the fault lines of the area (after Nguyen and Ho, 1988).

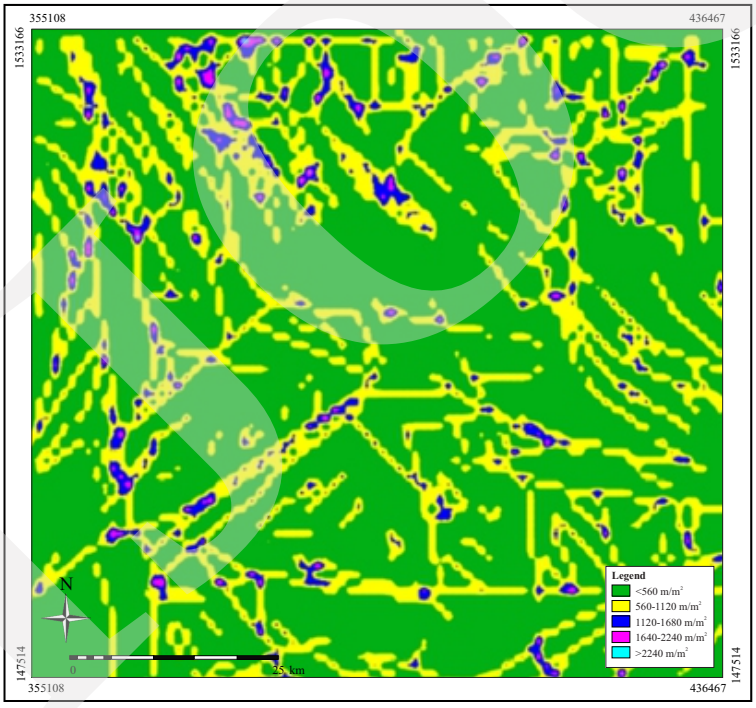

Figure 7. Density map of the geological fault lines.

The geophysical fault line (subsurface fault) map was created by digitizing the geophysical (magnetic) faults produced by Ameen Al-Qadasi (2014). The geophysical fault lines was converted into a density map, and the resultant map of the geophysical fault density was divided into five classes.

Annual Rainfall Data

Rainfall data for the past ten years has been collected from the National Water Resource Authority (NWRA Consultant, 2010). A spatial variation map of the rainfall was created with the moving average interpolation technique using ILWIS 3.4 software. The minimum and

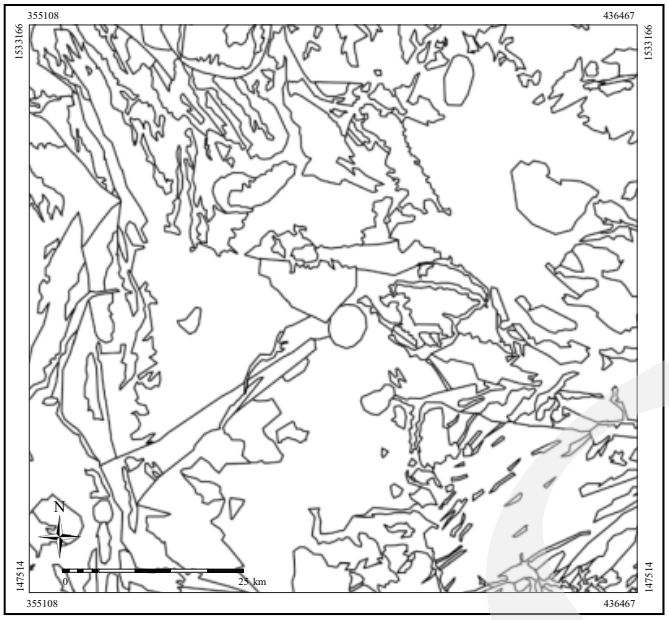

Figure 8. Contact map of the rock units.

maximum rainfalls received in the studied area were 550 and 850 mm, respectively. Precipitation is a very imperative portion of the water cycle, where its movement directs water from highlands to lowlands (Adiat *et al*., 2012). Rainfall is the major source of groundwater recharge that determines the amount available water to percolate into the groundwater systems.

Weighted Values of Factor Classes

For the identification of ground-water potential zones in the studied area, factors influencing the ground-water potential were prepared using thematic maps. A total of twelve parameters have been used in this analysis. The parameters are landuse, soil, lineament density, drainage density, slope, aspect, rock units, fault density, contact buffering, geophysical faults density, and rainfall. In this study, weighted values of the classes were assigned for each factor layer using three different methods as follows:

Manual Weighted Values

To investigate the origin, occurrence, movement, and situation of ground-water using GIS data based indirectly analysis of openly visible landscape features like geological, topographical, and geomorphological maps (Rajaveni *et al*., 2015). In this work, the twelve factors were used to create the groundwater potential zone map using GIS overlying operation technique. These factor maps were prepared to be suitable for GIS modeling technique. The twelve factors maps were created from the original data through several processes as mentioned in the above sections. Vector maps of these factors were converted into raster maps. The raster maps (factor maps) must be sliced into several classes. Each class from the different class in each factor map is assigned a weight value depending on its influence on surface water percolation, movement, and storage of groundwater. Before the overlying operation, the spatial values (weight values) must be given into the different classes within any factor map. According to Salwa (2015), Sciences (2013), and Sarah *et al.* (2006) the weighted value could be assigned between 1 and 5. In this section, the weight values are uniform ranks from 1 to 5, where 1 represents poor groundwater potential, and 5 represents excellent groundwater potential. In the present study the weighted sum analysis has been carried out by giving rank to individual parameters, and weights to individual themes, based on their degree of prospect and also the user experience as shown in Table 1. The resultant map from GIS overlying operation of the twelve

Table 1. Different Weighted Values of The Factor Maps MW= Manual Weighted; SW= Scaling Weighted, and XW= Matrix Weighted

Name of layer (factor)	Classes	Weight value			Name of layer (factor)	Classes	Weight value		
		MW	SW	XW			MW	SW	XW
Lineament	<785 m/m²	1	0.3	2.8	Elevation	<590 m	5	1.0	0.1
	785-1,570 m/m²	2	0.1	0.7		590-1,180 m	4	0.6	0.1
	1,570-2,355 m/m²	3	0.4	0.2		1,180-1,770 m	3	0.3	0.2
	2,355-3,140 m/m²	4	1.0	0.1		1,770-2,360 m	2	0.1	1.0
	>3,140 m/m²	5	0.7	1.4		>2,360 m	1	0.1	3.1
Drainage	<1,070 m/m²	5	0.6	0.0	Rainfall	<550 m/m3	1	0.1	2.9
	1,070 –2,140 m/m²	4	1.0	0.3		550-650 m/m3	2	0.3	1.1
	2,140-3,210 m/m²	3	0.1	0.0		650-750 m/m3	3	0.3	0.4
	3,210-4,280 m/m²	2	0.2	0.4		750-850 m/m3	4	0.5	0.2
	>4,280 m/m²	1	0.4	0.6		>850 m/m3	5	0.7	1.1
Fault	<560 m/m²	1	0.2	3.4	Geophysical fault	<400 m/m²	5	0.1	0.5
	560-1,120 m/m²	2	0.4	0.9		400-800 m/m²	4	0.1	0.1
	1,120-1,680 m/m²	3	0.3	0.2		800-1,200 m/m²	3	0.1	0.0
	1,680-2,240 m/m²	4	0.9	0.1		1,200-1,600 m/m²	2	0.7	1.7
	>2,240 m/m²	5	0.7	2.0		>1,600 m/m²	1	0.9	5.0
Landuse	Urban	1	0.7	0.0	Slope	<15°	5	0.9	0.4
	Vegetations	3	0.9	0.1		15° - 30 °	4	0.6	0.1
	Field-Plantation	4	0.4	0.9		30° - 45°	3	0.3	0.5
	Unused Area	5	0.1	5.0		45°-60°	2	0.2	1.6
Rock units	Basic Metavolcanics	1	0.1	1.8		>60°	1	0.2	3.9
	Marble and Metadolomite	1	0.1	4.1	Soil	Sands - Silts	5	1.0	2.5
	Paragneiss	2	0.1	2.5		Silts - Clays	3	0.3	3.2
	Amphibolites	1	0.0	5.0		Clays	1	0.2	1.3
	Migmatite	1	0.0	0.8	Contact	<30 m	5	0.9	4.2
	Syntectoic Gabbro	1	0.1	2.5		30-60 m	4	0.6	1.1
	Late to Posttectonic Gabbro	1	0.0	5.0		60-90 m	3	0.1	0.0
	Syntectonic Granite	2	0.2	5.0		90-120 m	2	0.1	0.1
	Amran Limestone	2	0.1	5.0		>120 m	1	0.1	0.4
	Tawilah Sandstone	5	0.9	1.9	Aspect	N	1	1.0	3.9
	Basalt	3	0.4	1.0		E	5	0.6	5.0
	Trachyite	3	0.1	0.1		NE	3	0.6	1.6
	Rhyolite and Dacite	3	0.1	0.2		SE	3	0.9	5.0
	Ignimbrite and Ashflow Deposits	5	0.1	1.7		S	5	0.5	2.2
	Granite	3	0.1	0.4		SW	4	0.5	3.8
	Granodiorite	2	0.1	1.0		W	4	0.2	2.6
	Syenite	3	0.1	1.3		NW	2	0.2	5.0
	Gabbro	1	0.0	0.3					
	Active Alluvium	5	0.1	2.0					
	Gravels	5	1.0	5.0					
	Loess and Ancient Dunes	3	0.3	4.8					
	Colluviums	3	0.3	0.3					

weighted factors was called groundwater potential map of manual weighted values.

Scaling Weighted Values

In this section, different techniques were used to create the weighted values of different classes of each factor. The matching option was used in this section, where the groundwater potential zone map produced by using manual weighted values was matched with the twelve factor maps. Before applying this technique, the manual potential map was classified into five classes, which are very low, low, moderate, high, and very high. The matching operation within ILWIS software was used to match the manual potential map with each factor map, separately. The statistical analysis of the matching histogram was obtained of each factor map. The numerical numbers of the histogram for the different classes within each factor were presented in relation to the classes of manual potential map. Then, the statistical analysis of defined classes of each factor map was used to determine values of the class as well the minimum, maximum, and difference among the classes within the factor map. After that, the scaling equation was applied to the values of the classes of the factor maps as bellow:

Defining the weighted values for each class within factor maps:

$$\text{Scaling Weighted Values} = \frac{DCV - Min.VCs}{Dif.VCs} \quad \ldots (1)$$

where:
DCV= Defined Class Value after crossed
Min. VCs= Minimum Value of Classes
Dif.VCs = Difference Value between max. and min. Classes

Then, the new values obtained from applying the above equation were assigned to the classes of each factor layer as shown in Table 1.

Matrix Analysis Weighted Values

In this section, the potential map produced by the manual weighted values was used to calculate the matrix weighted values. Hence, both of the cross and matching techniques were used to determine the numerical numbers of the classes within the factor map. The cross technique was used to identify the areas of classes of any factor map which only crossed with the areas of the manual potential map classes. The matching technique was used to calculate the defined area percentage of the manual potential map classes related to the factor map classes. The percentage values of the classes in each factor layers were calculated relating to the cross and matching techniques. Then the following equation was used to calculate the weighted values of the classes of each factor map as follows:

$$\text{Matrix Weighted Values} = \frac{(\frac{MCV}{CCV})*TCV}{100} \quad \ldots\ldots (2)$$

where:
MCV = Matching Class Value
CCV = Cross Class Value
TCsV = Total Class Values

GIS Model

For mapping the groundwater potential zones, a total of twelve parameters were used, such as landuse, soil, lineament density, drainage density, slope, aspect, rock units, fault density, contact buffering, geophysical fault density, and rainfall. The overlay process technique was used to create the potential zone map of the groundwater for the studied area based on the weighted values that assigned to the classes of the factor maps. The groundwater potential zone maps produced by this technique were classified into five categories which are very high, high, moderate, low, and very low.

The following equation was applied for the overlaying process of the twelve factors to produce the potential zone maps of the groundwater in this work.

$$\text{Potential map} = \Sigma\, fW / n \quad \ldots\ldots (3)$$

where:
fW = Factor Weighted Map
n = Number of Factor maps

Results and Discussion

The selection and preparation of the available twelve factors by several processing techniques to create the raster maps of all factors, then slice (classify) these maps into different classes based on their variations.

Landuse and Soil Maps

The landuse and soil maps produced from the ETM satellite images after color enhancement and classification techniques were shown in the Figures 9 and 10, respectively.

The vegetation and agricultural land have mostly clay to silt soil with high porosity and low permeability and decrease the infiltration rate of the water from the surface into the sub-surface where the aquifer of the water could be found. Whereas areas like wilds (unused areas) have mostly very coarse to medium sands including gravels and wadis deposits with a very high porosity and permeability may increase the flow and the infiltration rate of the water from the surface into sub-surface areas to recharge the water aquifer or groundwater table (Jensen, 1996; Manap 2013). The ground of the urban

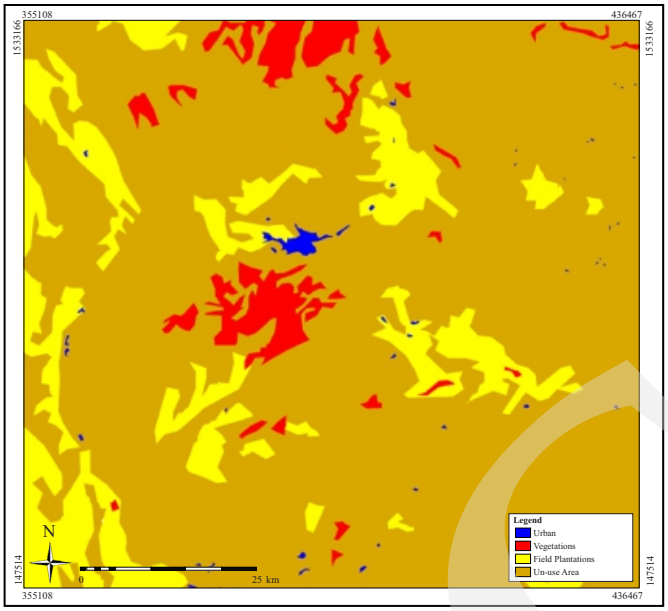

Figure 9. Landuse map extracted from coloured image of 432 band combination using the supervised classification technique.

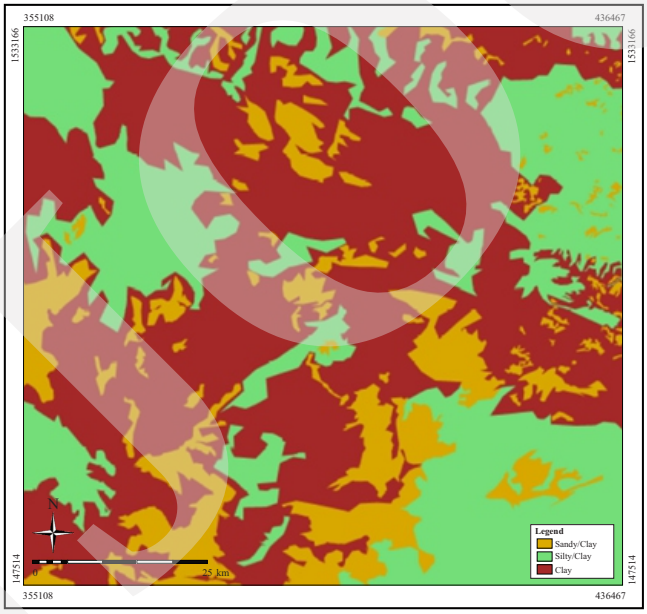

Figure 10. Soil map extracted from coloured image of 741 band combination using the supervised classification technique.

areas is always covered by man-made features like buildings and roads could decrease the infiltration rate into the sub-surface toward the groundwater table.

Elevation, Drainage and Lineament Maps

The raster map of the elevation steepness was classified into five categories based on the elevation reading. The altitudes were reclassified into five groups depending on their altitudes and ability to store and collect surface water. These classes as; < 590 m, 590-1180 m, 1180-1770 m, 1770-2360 m, and > 2360 m. The very low and low elevations (590 m and 590-1180 m) were referred to as the high percentage of the occurrence and movement of the surface water to recharge the groundwater. High and very high elevations (1770-2360, and > 2360 m) were awarded low

percentages according to their relation to groundwater recharge as shown in Figure 11.

The resultant map of the drainage network was shown in Figure 10. The minimum length of the drainage was 50 m, the maximum was 47.650 km and the sum was 385.106 km.

The drainages density map identified in the area was classified in to five categories as > 1600 m/m^2 (very high), 1200 – 1600 m/m^2 (high), 800 – 1200 m/m^2 (medium), 400 – 800 m/m^2 (Low) and < 400 m/m^2 (very low) in the study area as shown in Figure 12. The very high drainage density recorded at the volcanic mountains and near the mountain feet and very low drainage density recorded at the central rift floor area and some part of the flat lands. Groundwater potential is poor in areas with very high drainage density/ course as it lost majority in the form of runoff. On the

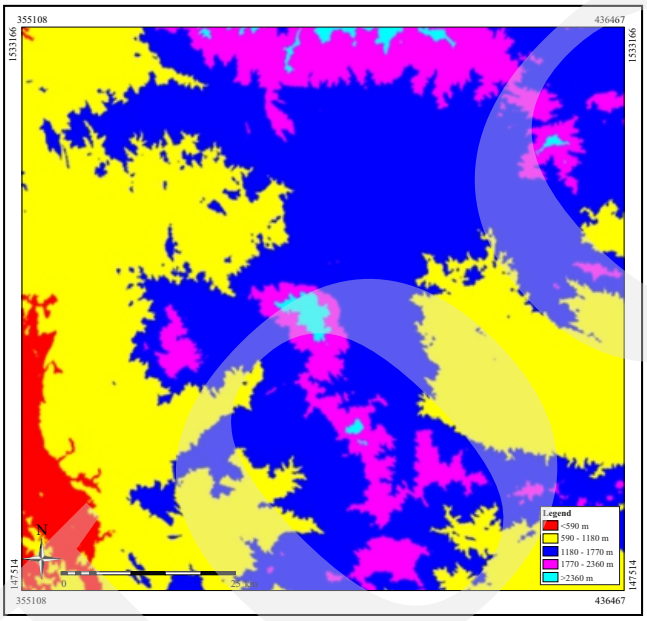

Figure 11. Elevation steepness created from DEM.

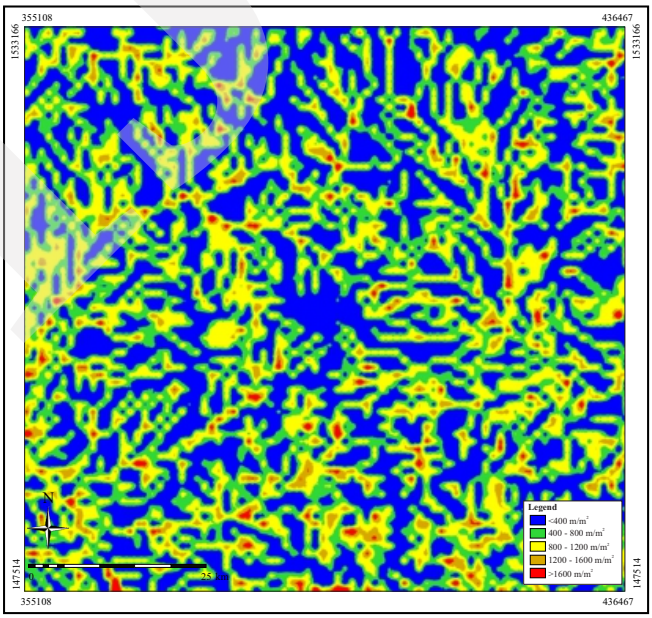

Figure 12. Density map of the drainage network of the studied area.

other hand, areas with low drainage density allow more infiltration to recharge the groundwater and, therefore, have more potential for ground water occurrence. The investigation and analysis of the drainage density map showed that high-drainage-density zone is located in the central toward the eastern and the western parts of the study area.

A total of 606 lineaments were identified in the area. Minimum lineament length is 294 m and the longest lineament observed was 25879 m. the total length of lineaments are 5253326 m. The lineament map of the study area indicates that the trends are predominantly along strikes of NW–SE and NE–SW directions (Figure 13).

The lineament density map identified in the area was classified in to five categories as > 3140 m/m^2 (very high), 2355 – 3140 m/m^2 (high), 1570 – 2355 m/m^2 (medium), 785 – 1570 m/m^2 (Low) and < 785 m/m^2 (very low) in the study area as shown in Figure 14. High lineament density areas are good for groundwater recharge and low lineament density are less suitable for groundwater recharge and discharges. The place having very high lineament density, the infiltration rate of the groundwater will be more, and the place were low lineament density, the infiltration rate of the groundwater will be less

The aspect identifies the downslope direction of the maximum rate of change in value from each cell to its neighbors. The areas having downslope directions of NW, SW and S were dominant in the area. This indicates that the groundwater potential is high in areas having downslope directions of NW, SW and S (Figure 15).

The identified slope category varies from 15° to 60° in the study area, and area classes like (<15°) gentle, (15°-30°) moderate, (30°-45°) high, (>45°) steep. Gentle slope (<15°) indicates the presence of very high groundwater potential zones where as steep slope (>45°) shows the presence of low groundwater potential zones as water runs rapidly off the surface and does not have sufficient time to infiltrate the surface, keeping other parameters constant as shown in the Figure 16.

Rock Units, Geological Faults, Contacts and Geophysical Faults

The rocks available in that area range from metamorphic rocks of Precambrian to the Quaternary alluvial deposit (Figure 6). Due to the porosity, permeability, hardness and fractures the movement of surface water into the groundwater is difficult in the metamorphic rocks and easy movement of the water in the unconsolidated

Figure 13. Lineament map extracted from gradient shader image of DEM.

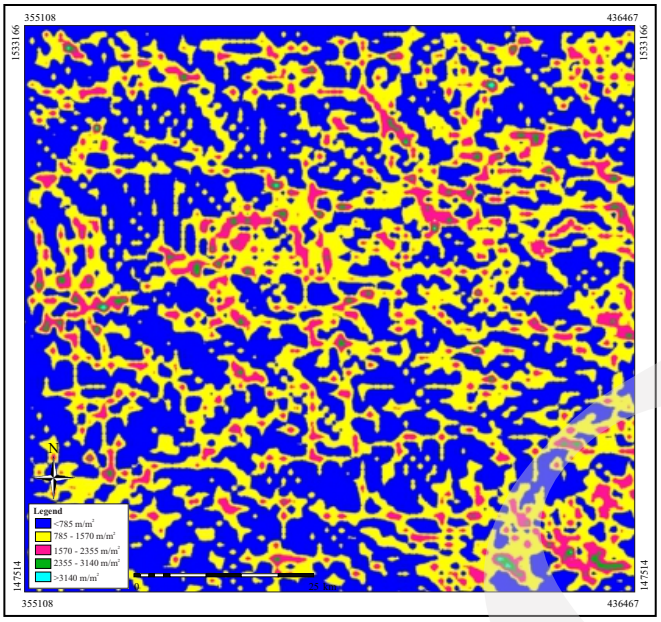

Figure 14. Density map of lineaments.

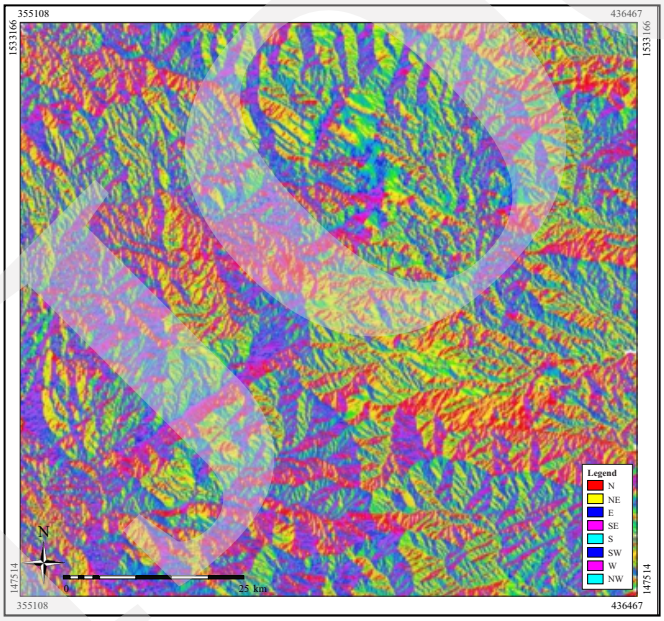

Figure 15. Aspect map created from DEM.

deposits, sandstones, basalts and granites, respectively.

A total of 388 faults were identified in the fault map of the study area. Minimum fault length is 208 m and the longest fault observed was 36999 m. The total length of lineaments are 2401495 m. The fault map shows the dominant directions in NW-SE and NE-SW (Figure 17). The geological fault density map was divided into five density classes based on their effect on groundwater occurrence; > 2240 m/m^2 (very high), 1640 – 2240 m/m^2 (high), 1120 – 1640 m/m^2 (medium), 560 – 1120 m/m^2 (low) and < 560 m/m^2 (very low) in the study area as shown in the Figure 7.

The contacts are the primary indicators of secondary porosity and also for potential sources of water supply. The contacts between the rock

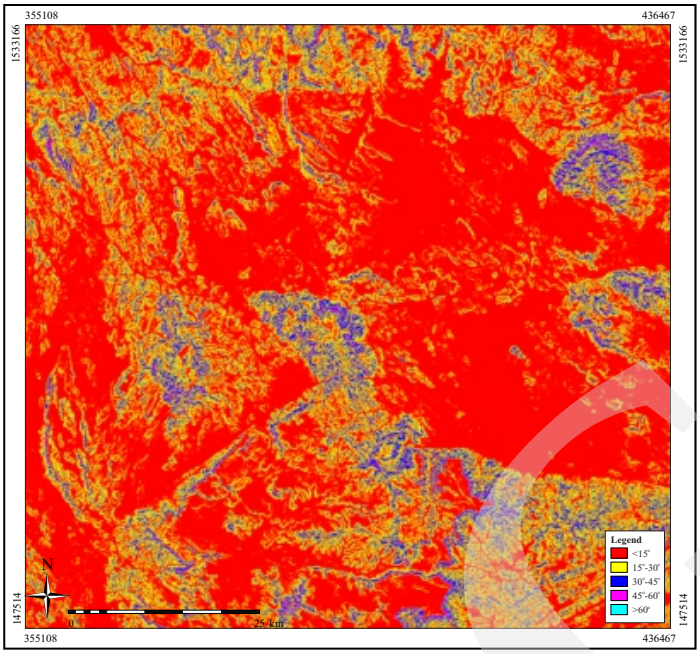

Figure 16. Slope map of the area.

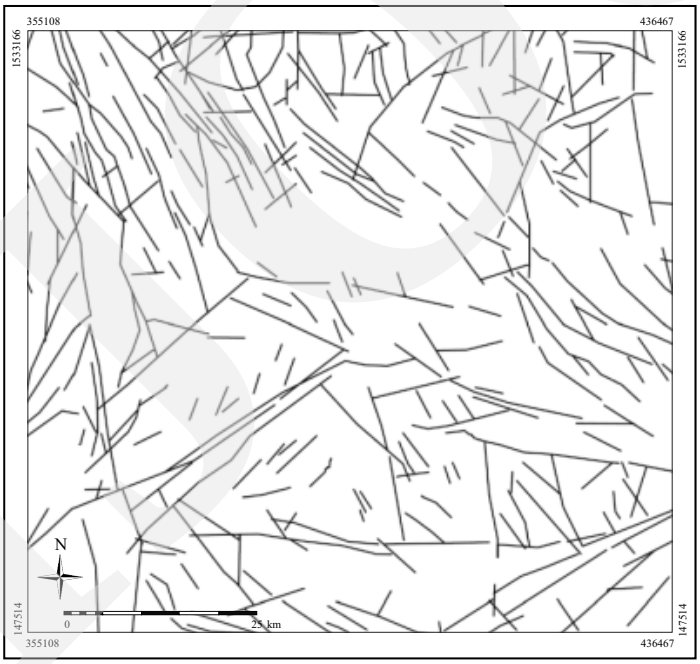

Figure 17. Geological faults of the area (Nguyen and Ho, 1988).

units may representing a zone of the structural weakness with high groundwater potential (Figure 8). The rock units contacts map was divided into five density classes based on their effect on groundwater occurrence; < 30 m (high), 30 – 90 m (moderate), and > 90 m (low) in the study area as shown in the Figure 18.

The subsurface geophysical faults (Figure 19) may played an important role in water movements and recharge the groundwater and occurrence. The geophysical density map identified in the area was classified into five categories as > 1600 m/m^2 (very high), 1200 – 1600 m/m^2 (high), 800 – 1200 m/m^2 (medium), 400 – 800 m/m^2 (low) and < 400 m/m^2

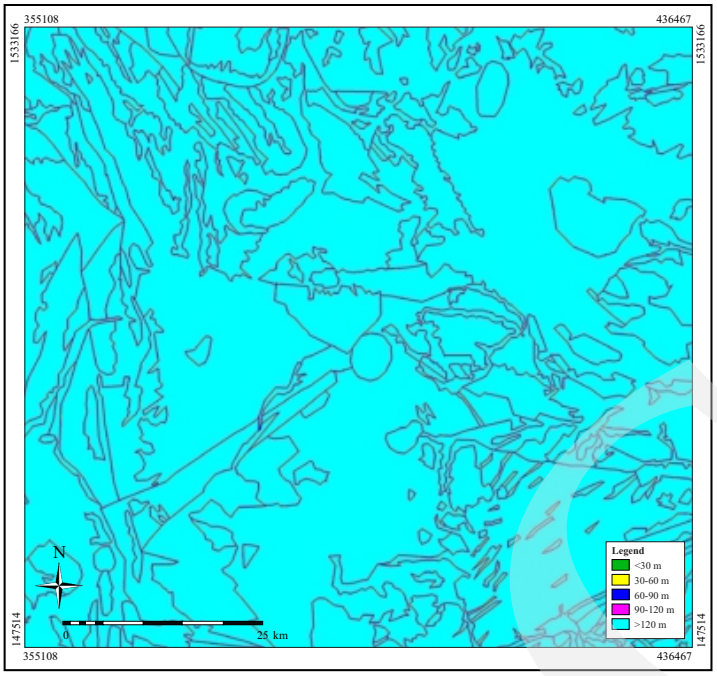

Figure 18. Buffering map of the rock unit contacts.

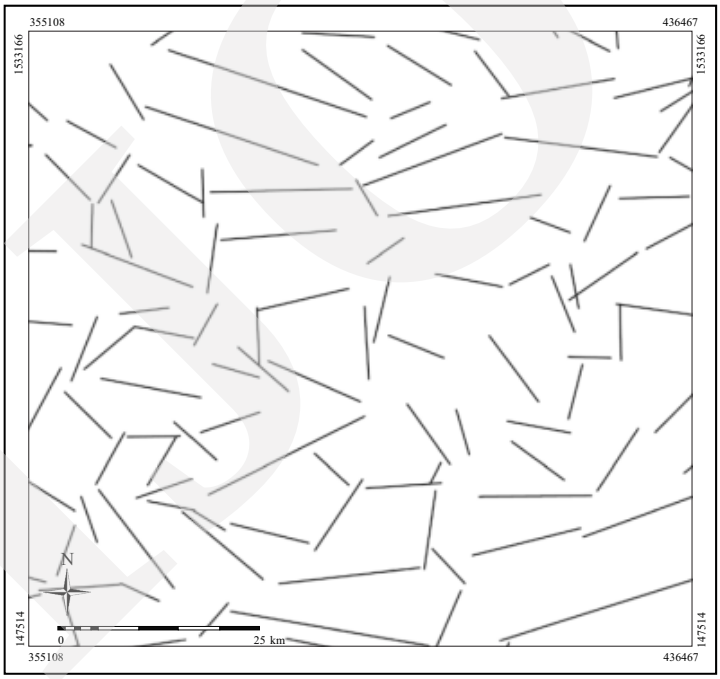

Figure 19. Geophysical fault lines of the area.

(very low) as shown in Figure 20. A high geological geophysical faults density indicates high secondary porosity, thus representing a zone with high groundwater potential. And a low geophysical fault density indicates poor secondary porosity, thus representing a zone with low groundwater potential.

Rainfall Map

The rainfall map was created and classified in to five categories; > 850 m/m^3 (very high), 750 – 850 m/m^3 (high), 650 – 750 m/m^3 (medium), 550 – 650 m/m^3 (low) and < 550 m/m^3 (very low) as shown in the Figure 21. The groundwater

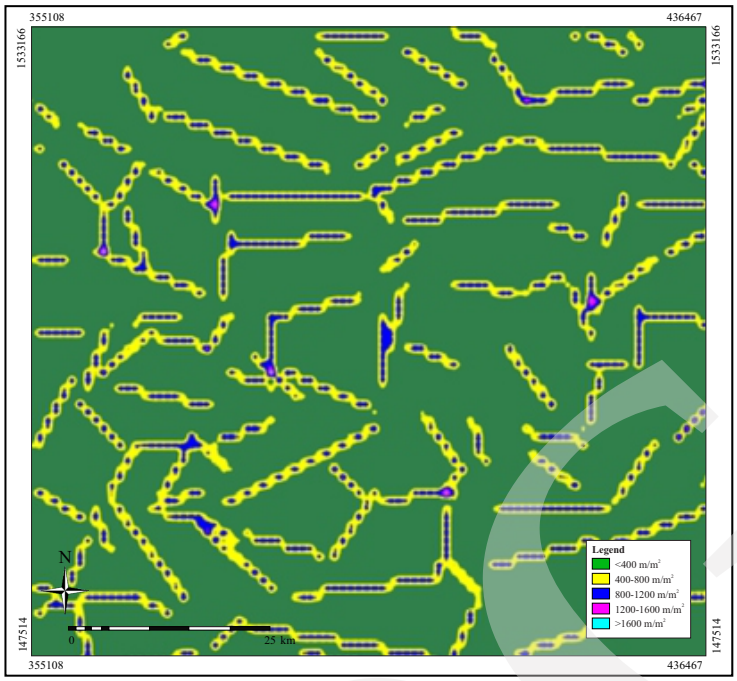

Figure 20. Density map of the geophysical fault lines.

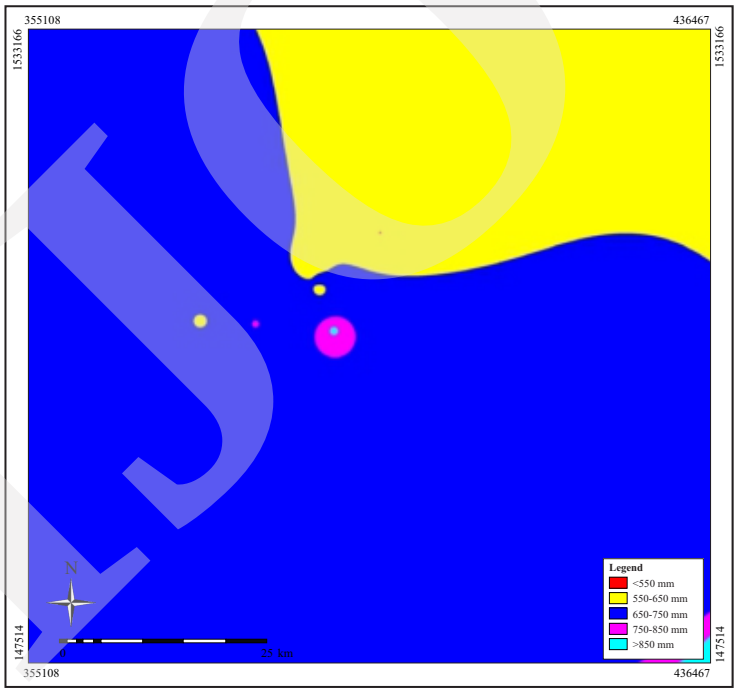

Figure 21. Average surface of the annual rainfall of the area (after NWRA Consultant, 2010).

potential is high in areas with very high annual rainfall. On the other hand, areas with low annual rainfall allow less infiltration to recharge the groundwater and, therefore, have less potential for ground water occurrence.

Groundwater Potential Zones Map

All the twelve factor maps were re-scaled by given same resolution. Geo-reference and coordinates the weighted values were given to the classes depend on the literature reviews of

same work, user experience and based on their respective contributions to the occurrence of groundwater.

A common measurement scale (weighted values) from 1 to 5 used in this work according to their effectiveness in the availability of groundwater. The final stage was to input all these maps to GIS overly model with potential Equation 3 of the ILWIS 3.4 software to overlay all these maps (layers) together using overlay technique to create map that identifies the potential groundwater zone's locations depend on the manual weighted values. The resultant map named as the groundwater potential zone map of the manual weighted values as shown in Figure 22. The potential map of the manual weighted values map was classified into five categories and shows the percentage of each class related to whole study area. The very low class with 7.34%, low class with 32.02%, moderate class with 40.68%, high class with 16.99% and very high class with 2.97%, respectively. Moreover, the very low zone represented by 223.8 m^2, 1280 m^2 for low zone, 3046m^2 for the moderate zone, 2412m^2 for the high zone and 552.6 m2 for the very high zone.

The first resultant potential map (groundwater potential map of the manual weighted values) of this work has been matched with the twelve factor maps used in this work, to determine the area percent of the different classes for each factor layer related to the groundwater potential map. On the other hand, this was done by using matching operation of the manual groundwater potential map with the twelve factor maps, separately. The results of this operation show the defined area percentage of the classes for each factor map out of the whole area of the manual potential map, then scaling Equation 1 was applied to find the weighted values of the classes in each factor map. The percentage values of the classes within each factor map were rescaled between 0 to 1 based on the scaling equation that mentioned above. Then, the factors maps were used to produce the second potential map using GIS overly model with potential Equation 3. The resultant values of this equation were given as weighted values of the different classes for the twelve factor maps. Then these maps again input to the GIS model for overlaying to create the second groundwater potential zone map as shown in Figure 23. The resultant map named the groundwater potential map of scaling weighted values. The resultant map of the second groundwater potential zones produced by using weighted values of scaling equation shows the percentage of each class related to whole study area. The very low class

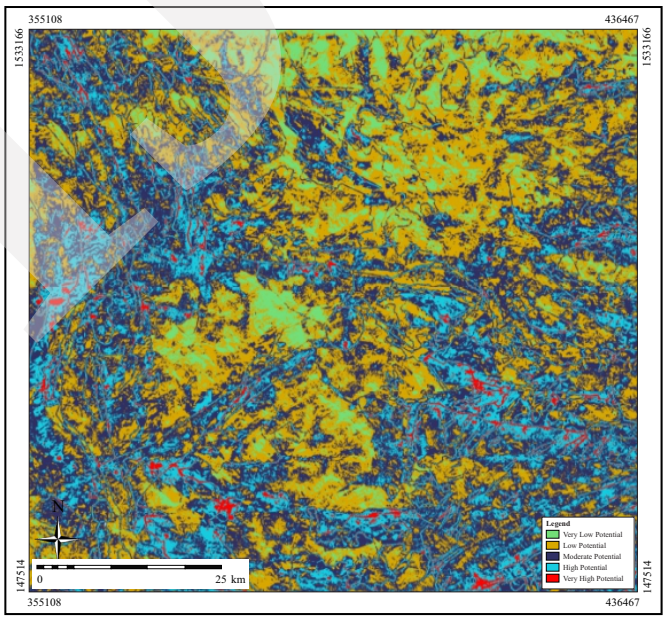

Figure 22. Groundwater potential map of manual weighted values.

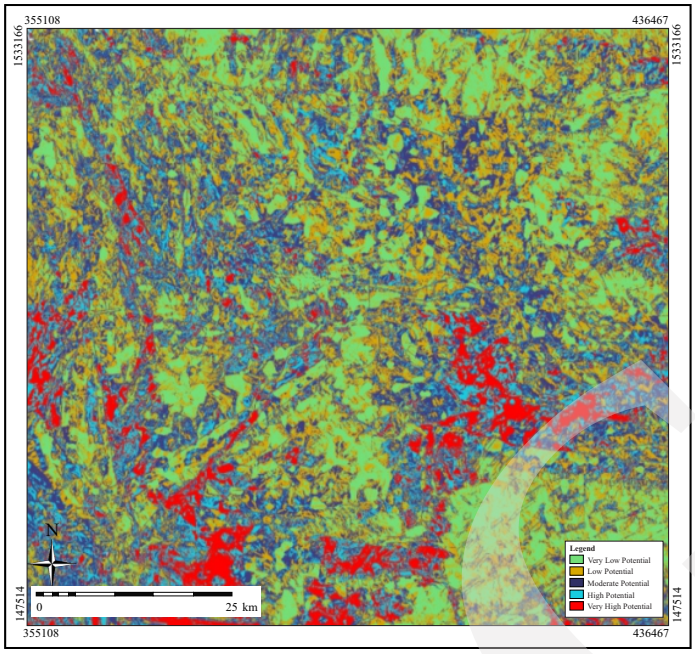

Figure 23. Groundwater potential map of scaling weighted values.

with 20.64%, low class with 27.07%, moderate class with 27.26%, high class with 15.17% and very high class with 9.83%, respectively. Whereas the very low zone represented 741.7 m^2 from the whole area, 1143.8 m^2 for low zone, 2055.7 m^2 for the moderate zone, 2024 m^2 for the high zone and 155.9 m^2 for the very high zone.

The third groundwater potential zones map was produced by given the new weighted values which create by statistical analysis of the matrix percentage of the different classes for each factor map itself related to the manual groundwater potential map using cross and matching operations. The third weighted value was created based on the cross operation to find the percentage value of the classes in each factor map from the total area of the manual potential map. Then the matching operation was done between each factor map and the manual potential map to find the percentage values of the potential map classes related to the classes of each factor map. The matrix Equation 2 was applied to find the weighted values of each factor map classes. Then, all factor layers with a new weighted valueare inputted into GIS model of overlay technique by ILWIS software using Equation 3. The resultant map of this section was shown in Figure 24 and named as the groundwater potential map of the matrix weighted values. The third groundwater potential zones map shows the percentage of each class related to the whole study area. The very low class with 13.73%, low class with 18.46%, moderate class with 25.63%, high class with 22.95% and very high class with 19.21%, respectively. The very low zone represented by 1037 m^2 in the area, 1392 m^2 for low zone, 1933 m^2 for the moderate zone, 1731 m^2 for the high zone and 1449 m^2 for the very high zone.

Results Evaluation

The groundwater potential zones maps mapped in this work will be evaluated in order to extract further information on the distribution and nature of the groundwater potential zones in the study area. The resultant three different groundwater potential zones maps that were created in this work by using different weighted values techniques of the twelve factor maps must be evaluated. The manual prospecting groundwater map (Figure 25) in the area prepared by NWRA 1997 [46] was used to evaluate the resultant maps of the groundwater potential zones by using matching technique and determining the percentage of matching led to evaluate the resultant maps in this work.

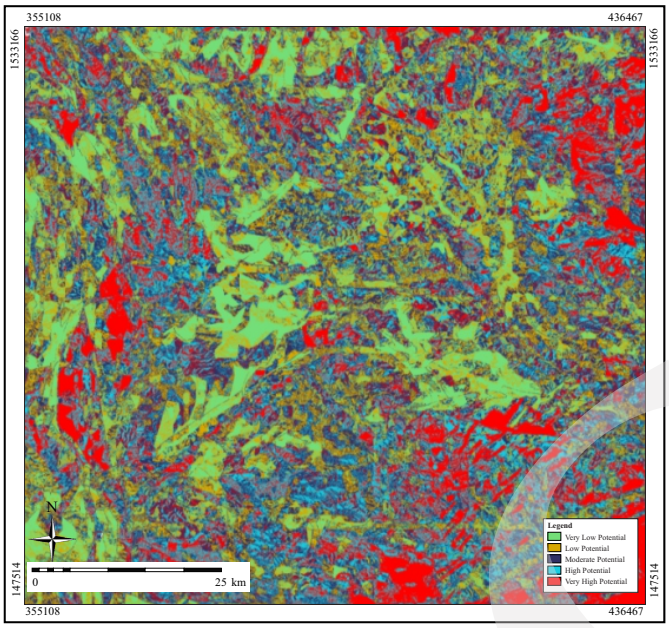

Figure 24. Groundwater potential map of matrix analysis weighted values.

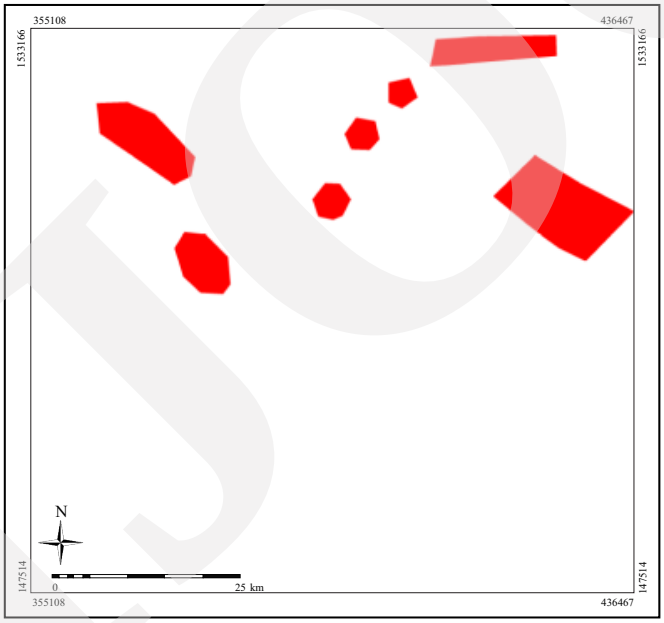

Figure 25. Prospecting groundwater aquifers in the area (after Al-Qadasi, 2014).

Hence, the three potential maps were matched with the map of the groundwater prospecting locations of the study area (pervious reference map), respectively. The result of this matching shows that, the third potential map has the highest percentage of the matching related to the very high potential zone of the groundwater in the area with 58.56 % in comparison with the second and first groundwater potential zones maps. The second and first groundwater potential zones maps have scored 27.95% and 13.49% percentage of matching with the reference map, respectively. As well, in terms of comparison it is clear to see that, the percentage value of the very high zone in the matrix potential map was higher than the percentage value of the very high zone within the manual and scaling potential maps, respectively. Moreover, the third groundwater

potential zone map shows more than six places of new prospecting areas for the groundwater in the Taiz region. The locations of these areas were NE corner, S-SW, W, NW corner, N, and some places in the central parts of the study area. This comparison indicates that weighted values of the factor layers based on the matrix statistical analysis technique was the best technique to prepare the weighted values of the factor maps to produce the groundwater potential zone map of the area using the overly technique process. And the best groundwater potential zones map was the potential map produced by GIS overly model of the weighted factors maps with matrix weighted values technique.

To determine the relationship between the factors and the groundwater potential maps created in this work, the area of each factor was calculated based on the very high potential zone area of the best groundwater potential map after using cross technique between factors and the best groundwater potential zones map as shown in the Table 2. It is clear to see that the rainfall seems to be the very important factor for influence and occurrence of the groundwater potential zones mapping in the area. The second important factor was the landuse. The other factors were the geophysical faults, slope, drainage elevation steepness, lineaments, geological faults, soil, contact, rock units and aspect, respectively.

Table 2. Factors and Their Percentage

No.	Name of factors	Percentage, %
1	Aspect	18.3
2	Contact	44.2
3	Elevation Steepness	61.7
4	Drainage	60.9
5	Geological Faults	46.6
6	Geophysical Faults	73.6
7	Landuse	87.4
8	Lineament	46.8
9	Rainfall	93.9
10	Rock Units	27.4
11	Slope	63.9
12	Soil	45.9

Conclusion

The advance statistical analysis of the some geo-factors provide useful information on the weighted values techniques to map the groundwater potential zones areas using GIS model. Various twelve factor layers were used and prepared from different data sources using several processes. The soil and landuse factors were prepared from Landsat-7 with color enhancement technique and supervised classification. The lineament, automatic drainage, slope, elevation steepness (topography) and aspect were derived from DEM. The rock units, geological faults, and contact created from previous geological map. Geophysical sub-surface faults also prepared from previous magnetic faults. The rainfall was generated from the previous annual rainfall reading. All these factors were created with the same resolution (30m) geo-reference and coordinate system, then converted into raster maps and classified (sliced) into different classes to be suitable for weighted values and GIS overly model technique.

There were three different techniques were used to calculate the weighted values which assigned to the classes of each factor. The manual weighted values was the first technique to determine the weighted values of the different classes within each factor. This was done based on literatures and user experience. The weighted values were rank between 1 to 5. The scaling weighted values technique was the second technique used to calculate the weighted values the different classes within each factor by applying the scaling equation. The variables of this equation were calculated using statistical analysis of the matching numerical values between the factors and manual potential maps. The resultant values were found between 0 to 1 and assigned to the different classes of each factor map. The matrix analysis weighted values was the third technique used to calculate the weighted values of the different classes within each factor. This was done by using statistical analysis of numerical values that resulted from matching and cross operations between the factors and manual potential maps. The matrix equation was used to calculate the weighted values of the classes of each factor map. The resultant values of this equation were found between 0.1 to 5 and assigned to the different classes of each factor map.

The GIS overlying operation model was used to created the different groundwater potential maps based on different weighted values techniques. The twelve factors with different weighted values were input into GIS model and used to create three different groundwater potential maps. The first potential map was created by using the manual weighted values technique and called the groundwater potential map of manual weighted values. This potential map was classified into five categories and shows the percentage of each class related to the whole area. The second result map was created by using the scaling weighted values technique and called the groundwater potential map of scaling weighted values. This map was classified into five types. The third potential map was resulted by using the matrix analysis weighted values technique and called the groundwater potential map of matrix weighted values. This map was classified into five classes. The percentage of each class related to the whole study area.

Based on the prospecting groundwater map (guessing, reference map) in the previous works of the study area was used to evaluate the three potential maps of the groundwater with different weighted values techniques produced in this research. This evaluation was done based on matching technique between only the very high potential zone of the three potential maps and the previous prospecting groundwater map. The results of this matching show that, the potential map of the matrix weighted values has the highest percentage of the matching related to the very high potential zone of the groundwater in the area with 58.56% in comparison with the scaling and manual weighted values groundwater potential maps. The scaling and manual groundwater potential zones maps scored 27.95% and 13.49%, respectively. Comparison of three different groundwater potential maps indicates that, the matrix analysis weighted values technique with statistical analysis produced the better results.

To determine the relationship between the factors and the groundwater potential maps; the area of each factor was calculated based on the very high potential zone area of the best groundwater potential map after using cross technique between factors and the best groundwater potential zones map. It is clearly to see that the rainfall seem to be the very important factor for influence and occurrence of the groundwater potential zones mapping in the area. The second important factor was the landuse. The other factors were the geophysical faults, slope, drainage elevation steepness, lineaments, geological faults, soil, contact, rock units and aspect, respectively.

Acknowledgement

The authors express appreciation to Taiz University, Yemen and Universiti Malaysia Sabah, Malaysia for all their support in this research.

References

Abdullah, A., Akhir, M.J., and Abdullah, I., 2010. Automatic mapping of lineaments using shaded relief images derived from digital elevation model (DEMs) in The Maran -Sungai Lembing area, Malaysia. *Electronic Journal of Geotechnical Engineering,* 15, p.949-957.

Abdullah, A., Nassr, S., and Ghaleeb, A., 2013. Remote Sensing and Geographic Information System for Fault Segment Mapping, A Study from Taiz Area, Yemen. *Journal of Geological Research,* 16. DOI: 10.1155/2013/201757.

Adiat. K.A.N., Nawawi, M.N.M., and Abdullah, K., 2012. Assessing the accuracy of GIS based elementary multicriteria decision analysis as a spatial prediction tool, A case of predicting potential zones of sustainable groundwater resources. *Journal of Hydrology,* 440-441, p.75-89. DOI: 10.1016/j.jhydrol.2012.03.028

Al-Qadasi, A., 2014. Interpretation of aeromagnetic data in terms of surface and subsurface geologic structures, southwestern Yemen. *Arabian Journal of Geosciences*, DOI 10.1007/s12517-013-1238-1.

Aneesh, R. and Deka, P.C., 2015. Groundwater potential recharge zonation of Bengaluru urban district, a GIS based analytic hierarchy process (AHP) technique approach. International Advanced Resources, *Journal of Science Engineering Technology,* 2 (6), p.129-136. DOI: 10.17148/IARJSET.2015.2628

Avtar, R., Singh C.K., Shashtri, S., Singh, A., and Mukherjee, S., 2010. Identification and analysis of groundwater potential zones in Ken-Betwa River linking area using remote sensing and geographic information system. *Geocarto International,* 25 (5*)*, p.379-396. DOI: 10.1080/10106041003731318

Babu, K.J., Sreekumar, S., and Arish, A., 2016. Implication of drainage basin parameters of a tropical river basin of South India. *Apply Water Science*, 6, p.67-75. DOI: 10.1007/s13201-014-0212-8

Brockmann, C.E., Fernandez, A., Ballon, R., and Claure, I.I., 1977. Analysis of Geological Structures Based on Landsat-1 Images. In: Smith, W.L. (eds.) *Remote Sensing Applications for Mineral Exploration:* p.292-317. Dowden. Hutchinson & Ross. Strondsberg. PA.

Chen, X. and Campagna, D.J., 2009. Remote Sensing of Geology. *In*: *The Sage Handbook of Remote Sensing* (Thousand Oaks, CA: Sage), p.328-340. DOI: 10.4135/9780857021052

Das, A., Mondal, M., Das, B., and Ghosh, A.R., 2012. Analysis of drainage morphometry and watershed prioritization in Bandu Watershed, Purulia, West Bengal through remote sensing and GIS technology, a case study, *International Journal of Geomatics and Geosciences.* 2 (4), p.995-1013.

Encyclopedia, 2022. *Water*. http:// www.water-encyclopedia.com/Tw-Z/Uses-of- Water.html.

GSY (Geological Survey of Yemen), 1991. *Geological sheet map of Taiz Governorate with 1: 250,000 scale*.

Glass, N., 2010. The Water Crisis in Yemen: Causes, Consequences and Solutions. Global-Majority *E-Journal,* 1 (1), p.1730.

Gupta, M. and Srivastava, P.K., 2010. Integrating GIS and remote sensing for identification of groundwater potential zones in the hilly terrain of Pavagarh, Gujarat, India. *Water International,* 35 (2), p.233-245. DOI: 10.1080/02508061003664419

Gupta, R.P., 2013. *Remote Sensing Geology* (Berlin, Heidelberg: Springer Berlin Heidelberg).

Horton, R.E., 1945. Infiltration and runoff during the snow-melting season, with forest- cover. Eos, Transactions, *American Geophysical Union,* 26 (1), p.59-68.

Isnain, Z. and Mokthar, H.E., 2022. Mapping the Groundwater Potential Areas by Using the GIS Method in Kg Samawang, Sandakan, Sabah, Malaysia. *IOP Conference Series Earth and Environmental Science*, 1103 (1), 012017 DOI:10.1088/1755-1315/1103/1/012017

Isnain, Z. and Musta, B., 2022. *IOP Conference Series Earth and Environmental Science, 1103 012021.*

Jensen, J.R., 1996. *Introductory Digital Image Processing, 2nd Edition*, Prentice Hall Inc., U.S.A.

Jensen, J.R., 2005. *Introductory Digital Image Processing*. Pearson Prentice Hall, Upper Saddle River.

Jha, M.K., Chowdhury, A., Chowdary, V.M., and Peiffer, S., 2007. Groundwater management and development by integrated remote sensing and geographic information systems: prospects and constraints. *Water Resource Management,* 21, p.427-467. DOI:10.1007/s11269-006-9024-4

Kumar, M.G., Agarwal, A.K., and Bali, R., 2008. Delineation of potential sites for water harvesting structures using remote sensing and GIS. *Journal of the Indian Society of Remote Sensing,* 36, p.323-334. DOI:10.1007/s12524-008-0033-z

Kumar, P., Herath, S., Avtar, R., and Takeuchi, K., 2016. Mapping of groundwater potential zones in Killinochi area, Sri Lanka, using GIS and remote sensing techniques. Sustain. *Water Resource Management.* 2, p.419-430. DOI: 10.1007/s40899-016-0072-5

Manap, M.A., 2013. A knowledge-driven GIS modeling technique for groundwater poten-

tial mapping at The Upper Langat Basin, Malaysia. *Arabian Journal of Geosciences,* 6 (5), p.1621-1637. DOI: 10.1007/s12517-011-0469-2

Nassr, S. and Abullah, A., 2015. The Delineation of Linear Features from Different Image Resolutions Using Edge Modelling Technique in the Al-Mawasit Area, Taiz, Yemen. *American Journal of Geophysics, Geochemistry and Geosystems.* 1 (1), p.7-18.

Nguyen, P.T. and Ho, D., 1988. Multiple source data processing in remote sensing. In: Muller, J.P. (eds). *Digital Image Processing in Remote Sensing*, p.153-176. Philadelphia: Taylor & Francis Ltd.

NWRA Consultants, 1997. National Water Resource Authority (NWRA) *Taiz water supply pilot project. UNDP/NWRA /DDSMS Programme YEM 97/200 Sustainable Water Resource Management.*

NWRA Consultants, 2010. *Annual rainfall reading data of Taiz region. Sustainable Water Resource Management.*

Pradhan, B., Singh, R.P., Buchroithner, M.F., 2006. Estimation of stress and its use in evaluation of landslide prone regions using remote sensing data. *Advances in Space esearch,* 37, p.698-709. DOI:10.1016/j.asr.2005.03.137

Pradhan, B., 2009. Flood Susceptible Mapping and Risk Area Delineation Using Logistic Regression, GIS and Remote Sensing. *Journal of Spatial Hydrology,* 9, p.1-18.

Rajaveni, S.P., Brindha, K., and Elango, L., 2015. Geological and geomorphological controls on groundwater occurrence in a hard rock region. *Applied Water Science*, 7 (3), p.1-13. DOI:10.1007/s13201-015-0327-6

Rao, S.Y. and Jugran, D.K., 2003. Delineation of groundwater potential zones and zones of groundwater quality suitable for domestic purposes using remote sensing and GIS. *Hydrology Science Journal,* 48, p.821-833. DOI: 10.1623/hysj.48.5.821.51452

Ross, R.R. and Beljin, M.S., 1994. MODRISI: A PC Approach to GIS and Groundwater Modeling. *Seminar Publication, National Conference on Environmental Problem- Solving with Geographic Information Systems. Cincinnati, Ohio.*

Ruiz, L., Varma, R., Kumar, M., Sekhar, M., Maréchal, C., Descloitres, M., Riotte, J., Kumar, S., Kumar, C., and Braun, J., 2010. Water balance modelling in a tropical watershed under deciduous forest (Mule Hole, India); regolith matric storage buffers the groundwater recharge process. *Journal of Hydrology,* 380 (3-4), p.460-472. DOI: 10.1016/j.jhydrol.2009.11.020

Salwa. F., 2015. An overview of integrated remote sensing and GIS for groundwater mapping in Egypt. *Ain Shams Engineering Journal*, 6 (1), p.1 -15. DOI: 10.1016/j.asej.2014.08.008

Sarah, O., Tweed & Marc, Leblanc & John, A., Webb & Maciek, W. Lubczynski, 2006. Remote sensing and GIS for mapping groundwater recharge and discharge areas in salinity prone catchments, in outheastern Australia. *Hydrogeology Journal*, Springer-Verlag. 15 (1), p.75-96. DOI: 10.1007/s10040-006-0129-x

Suganthi, S., Lakshmanan, E., Subramanian, S.K., 2013. *Groundwater potential zonation by Remote Sensing and GIS techniques and its relation to the Groundwater level in the Coastal part of the Arani and Koratalai River Basin, Southern India,* 17 (2*)*, p.87-95.

Shaban, A., Khawlie, M., and Abdallah, C., 2006. Use of remote sensing and GIS to determine recharge potential zone: The case of Occidental Lebanon; *Hydrogeological Journal,* 14, p.433-443. DOI: DOI:10.1007/s10040-005-0437-6

Shekhar, S. and Pandey, A.C., 2014. Delineation of groundwater potential zone in hard rock terrain of India using remote sensing, geographical information system (GIS) and analytic hierarchy process (AHP) techniques. *Geocarto International,* 30, p.402-421. DOI: DOI:10.1080/10106049.2014.894584

Singhal, B.R.P. and Gupta, R., 1999. *Applied Hydrogeology of Fractured Rocks.* Springer Dordrecht, Springer Science + Business

Media Dordrecht 1999. DOI: 10.1007/978-94-015-9208-6.

Solomon, S. and Ghebreab, W., 2008. Hard-rock hydrotectonics using geographic information systems in the central highlands of Eritrea: implications for groundwater exploration. *Journal of Hydrology,*349 (1), p.147-155. DOI: DOI:10.1016/j.jhydrol.2007.10.032

Sreedevi, P.D., Subrahmanyam, K., and Shakeel, A., 2005. The significance of morphometric analysis for obtaining groundwater potential zones in a structurally controlled terrain. *Environmental Geology,* 47 (3), p.412-420. DOI: 10.1007/s00254-004-1166-1

Stafford, D.B., 1991. *Civil engineering applications of remote sensing and geographic information systems*. New York (NY): ASCE.

Thapa, R., Gupta, S., Guin, S., and Kaur, H., 2017. Assessment of groundwater potential zones using multi-influencing factor (MIF) and GIS: A case study from Birbhum District, West Bengal. *Applied Water Science,* 7, p.4117-4131. DOI: 10.1007/s13201-017-0571-z

Todd, D.K.M.L., 2005. *Groundwater hydrology, 3rd edition*. Wiley, *Nation Journal*, pp. 636.

Waikar, M,L. and Nilawar. A.P., 2014. Morphometric analysis of a drainage basin using geographical information system: a case study. *International Journal Multi-discipline Current Resources,* 2, p.179-184.

Wakgari, F., 2010. The hydrogeology of Adama-Wonji Basin and assessment of groundwater level changes in Wonji wetland, Main Ethiopian Rift: results from 2D tomography and electrical sounding methods. *Environmental Earth Sciences,* 62 (6), p.1323-1335. DOI : 10.1007/s12665-010-0619-y